Impact of operational details and temporal representations on investment planning in energy systems dominated by wind and solar

Helistö, Niina; Kiviluoma, Juha; Morales-España, Germán; O'Dwyer, Ciara

Published in:
Applied Energy

DOI:
10.1016/j.apenergy.2021.116712

Published: 15/05/2021

Document Version
Publisher's final version

Applied Energy 290 (2021) 116712

Contents lists available at ScienceDirect

Applied Energy

journal homepage: www.elsevier.com/locate/apenergy

Impact of operational details and temporal representations on investment planning in energy systems dominated by wind and solar

Niina Helistö [a,*], Juha Kiviluoma [a,c], Germán Morales-España [b], Ciara O'Dwyer [c]

[a] Smart Energy and Built Environment, VTT Technical Research Centre of Finland Ltd, FI-02044 VTT Espoo, Finland
[b] Energy Transition Studies, Netherlands Organisation for Applied Scientific Research (TNO), Amsterdam, The Netherlands
[c] School of Electrical and Electronic Engineering, University College Dublin, Ireland

A R T I C L E I N F O

Keywords:
Energy system optimization
Operational constraints
Power system planning
Representative periods
Time series reduction
Unit commitment
Variable renewable energy

A B S T R A C T

Planning of future energy systems with higher prevalence of wind and solar energy requires a careful representation of the temporal and operational characteristics of the system in the investment planning model. This study aims to identify the aspects that should be considered when selecting the representation for a particular system. To demonstrate the impacts that various model representations have in terms of model accuracy and computational effort, we carry out case studies on two test systems implemented within the Backbone energy systems modelling framework. The results show that the temporal and operational representations have different benefits and weaknesses in different system types. The findings provide general guidelines on the relative importance of different model details, depending on the characteristics of the system under study. For example, some temporal sampling strategies can better capture long-term storage needs, while others are more suitable for short-term storage modelling. Likewise, solar-dominated and wind-dominated systems differ in their methodological requirements. Furthermore, the interactions between energy sectors and the operational limits of the technologies for sector coupling should be correctly captured, as they significantly impact on the value of different technologies and their flexibility. Finally, we recommend testing several temporal and technical representations for each particular system in order to ensure the feasibility of the selected method for that purpose. The findings and recommendations inform energy system modellers about improvements that will facilitate higher quality planning results.

1. Introduction

Future energy systems will be increasingly based on weather-dependent renewable energy sources that are, by nature, variable and uncertain. They increase power system flexibility needs in different time scales, from less than a second to months and years, and in different spatial scales, from local to country- or even continent-wide. Higher flexibility needs mean that a greater ability is required from the system to respond to changes in demand and supply. Various technologies exist and are being developed that can provide flexibility, including, for example, flexible thermal power plants, reservoir and pumped-storage hydropower plants, batteries, power-to-gas facilities, power-to-heat facilities combined with thermal storage in district heating grids, as well as various demand response from industry and smaller consumers. Curtailment of the weather-dependent renewable energy sources and increased use of interconnections also provide flexibility. Estimating the value of these technologies in energy systems requires planning models that can correctly capture the temporal, spatial, and technological diversity.

1.1. Strategies to lower the computational burden in large-scale models

The temporal, spatial, and technological diversity increases the model size and complexity, and solving the large-scale models can easily become very slow or even impossible. Apart from taking advantage from the increasing evolution of software (solvers) and hardware (computers), the computational burden of the models can also be lowered by manipulating the original planning model. This model manipulation is mainly (1) reformulating the model,[1] (2) applying decomposition

Abbreviations: CCS, carbon capture and storage; CHP, combined heat and power; FCR, frequency containment reserve; FFR, fast frequency reserve; FRR, frequency restoration reserve; LP, linear programming; MILP, mixed-integer linear programming; NGCC, natural gas combined cycle; O&M, operational and maintenance; OCGT, open cycle gas turbine; PV, photovoltaic; RD, regular decomposition; RoCoF, rate-of-change-of-frequency; RS, random sampling; RTPV, rooftop photovoltaic; RTS-GMLC, Reliability Test System Grid Modernization Lab Consortium; VRE, variable renewable energy

* Corresponding author.
E-mail address: niina.helisto@vtt.fi (N. Helistö).

[1] Reformulation can provide significant computational savings especially for mixed-integer linear programming (MILP) models.

https://doi.org/10.1016/j.apenergy.2021.116712
Received 9 October 2020; Received in revised form 18 February 2021; Accepted 19 February 2021

methods, (3) simplifying the formulation, and (4) using aggregation methods. In both reformulation and decomposition methods, the details of the formulation are not affected. Simplifying or even ignoring some constraints reduces the model size but will naturally also decrease the level of detail. The same happens when using aggregation methods, which can be applied to the temporal, spatial, and technological part of the model. This study focuses on the impact of simplification and aggregation methods — more precisely, alternately including and ignoring different operational details and testing different ways to aggregate, cluster, and sample the temporal dimension.

1.2. Capturing temporal variability

As the volume of variable renewable energy (VRE) in energy systems continues to grow, it is increasingly important to consider a wide range of different operational situations and challenges when planning investments. Ideally, planning models should include time series spanning a full year or more, with a high resolution, e.g., at least hourly. Furthermore, it is important to retain chronological and spatial–temporal correlations in the time series to correctly model storage levels and realistic weather situations. To keep large-scale models with high temporal detail computationally feasible, modellers have to make choices for reducing the detail.

One option to reduce the temporal detail is to select representative periods, e.g., days or weeks, from the time series. The periods can be selected by using, for example, clustering [1], optimization [2], sampling [3], heuristics [4], or brute force methods [5]. Interestingly, Poncelet et al. [2] and Helistö et al. [6] showed that random sampling with a sufficient number of iterations can have similar or even better performance compared to other methods. Selecting representative periods by default means that extreme periods will not be included in the model. However, extreme periods, such as the peak of the net load time series (load less VRE generation), can be separately included in the model, for example, through multi-stage approaches [7]. The weight of the extreme periods should be determined carefully and it becomes increasingly important when using multi-year time series, as noted by Yeganefar et al. [8], who employed a self-organizing map clustering method that could be further improved to consider the impact of new VRE investments on the net load and the position of the extreme periods. Furthermore, in some systems, peak ramps – especially of net load – can also be important extreme periods to consider. The optimal number of representative days or weeks in the model depends on the system characteristics and computational resources. In a recent study, Helistö et al. [6] demonstrated that at least seven (including one extreme) weeks are needed for a multi-region power system model to confidently obtain total system costs close to the cost results based on a full year model.

Another option to reduce the temporal detail is simply reducing the temporal resolution in the model, e.g., by aggregating 1-h time steps into 2-h time steps [4]. However, this aggregation can lose important short-term variations in the time series. A hybrid approach is to select which time steps retain the original high resolution, and which could be aggregated together in order to reduce the model size [9]. Wogrin et al. [10] compared this chronological time-period clustering method with an enhanced representative periods approach [11] that creates continuity in the temporal horizon by using a transition matrix and a column vector containing the representative period assignments. The results showed that the chronological time-period clustering method can better handle long-term storage dynamics in power system operation models, while the enhanced representative periods approach better predicts short-term storage production. Other methods for modelling long-term storage also exist, such as applying a storage description based on inter-period and intra-period states [12]. One of the objectives in the present study is to compare the representative weeks method (with cyclic and continuous storage state modelling) with a temporal representation where the resolution varies across the whole time horizon, and to find out how these approaches perform in investment planning.

1.3. Capturing operational flexibility

The detail of the investment optimization model depends not only on its temporal representation but also on its operational detail. Operational detail includes, for example, the representation of the online status of power plants,[2] which can be represented using online variables that follow the start-up and shutdown decision variables through the so-called unit commitment constraints. The online decision variables can be binary in order to solve an individual unit commitment, where each power plant is represented separately, or they can be integer to solve a clustered unit commitment, which aggregates similar power plants and reduces the model size [13]. To obtain a significant computational advantage, the binary or integer variables can be relaxed, i.e., treated as continuous variables, thus converting the initial MILP problem into a linear programming (LP) problem. However, the trade-off for each simplification is the reduction in the accuracy of the results.

Various literature shows that modelling (binary or integer) online variables and unit commitment constraints is important for capturing the actual flexibility of the system with growing volumes of VRE, although not as important as improving the temporal representation and considering reserve requirements (see e.g. a case study of India [14] and a literature review [15]). The need for base load power plants is decreasing, and flexible power plants that can start up and shut down easily and that have low minimum loads are becoming more important. These impacts cannot be adequately captured without online variables. However, as the share of VRE grows further and if storage technologies become more widespread, the role of conventional power plants may decrease so much that modelling online variables can become less significant [16].

Reserve sizing and allocation, as well as other ancillary services, are an essential part of power system operations. Reserve products are used to balance those deviations between consumption and production that are not already balanced in energy markets, for example due to uncertain events. In Europe, ENTSO-E (European Network of Transmission System Operators for Electricity) has categorized reserve products according to their purpose: frequency containment reserve (FCR), frequency restoration reserve (FRR), and replacement reserve (RR)[3] [17]. Some transmission system operators have also proposed and started to procure fast frequency reserve (FFR) for handling low-inertia situations [18]. FFR from wind power plants, PV units, and battery storage systems can help improve system stability, but a sufficient number of online synchronous generators may still be required in order to maintain a minimum inertia level and ensure an acceptable rate-of-change-of-frequency (RoCoF) immediately after a large disturbance [19]. Disregarding inertia constraints in generation expansion planning can result in additional system costs [20], although the increase in costs was fairly modest in the illustrative case study. As an alternative to the inertia of synchronous generators, studies have proposed using synchronous condensers [21] and grid forming inverters [22]. However, further technical and techno-economic research as well as experimentation are needed on both concepts before their wide deployment. Initial studies indicate that in inverter-based systems, it is generally adequate that 10%–30% of the total power units are connected through grid forming inverters [19].

Wind and solar power plants can increase the fast ramping needs of the system, although they can also be part of the solution by providing flexibility through scheduled curtailment [23] and ancillary

[2] The representation of the online status may be important especially for conventional power plants with minimum load levels and efficiencies that depend on the load level.

[3] FCR is available to contain system frequency after the occurrence of an imbalance, FRR is for restoring system frequency to the nominal value and for releasing activated FCR back into use, and RR is for restoring or supporting the required level of FRR to be prepared for additional system imbalances.

services [24]. Nevertheless, in order to maintain the balance between production and consumption, and leverage the available weather-dependent energy, other power plants may need to change their production faster than has been required in the past. Another option is that flexible loads provide a fast response through changes in their consumption. In both cases, it is important that the resolution of the model is high enough to capture the possible ramps in the weather-dependent generation and the ramping limits of other power plants and flexible loads. This may even require sub-hourly resolutions, at least in small systems like in Ireland [25]. In hourly models, ramping constraints often have an insignificant impact on results [26], although the opposite can also happen if considering very inflexible units with stringent ramping limits [27]. Priesmann et al. [28] also conclude that modelling ramping rates improves the accuracy and robustness of power system optimization models. On the contrary, according to their results, partial load efficiency implementations have little influence on the accuracy of power system optimization models, and minimum loads, start-up costs, and minimum down times should only be included jointly.

While the previous studies have focused on certain elements of the power or energy system models, the present study covers a wider range of operational details and presents a more comprehensive comparison, including features such as combined consideration of FFR and inertia requirements, different storage dynamics, and flexibility from sectoral integration.

1.4. Capturing spatial and sectoral integration

In a power grid, production and consumption need to be balanced at every grid node. Evidently, the spatial resolution of the model and the detail of power flow calculation play an important role in investment planning, and also greatly increase the computational demand. In the present study, we disregard nodes and transmission constraints, allowing increased focus on the computation of other operational aspects in high detail.

In order to further decarbonize the energy system and benefit from all available flexibility options, it is paramount to consider integration of different energy sectors. Since most carbon free primary energy sources generate power, energy system electrification is considered one of the most promising pathways to reduce carbon emissions [29]. In some countries, power and heat sectors have long been coupled through combined heat and power (CHP) plants, and also through heat pumps and electric boilers. CHP plants can provide flexibility through flexible output ratios [30], and heat pumps and electric boilers offer flexibility when combined with thermal storage [31] or with alternative sources of heat production [32]. Large thermal storage facilities are often a cost-effective way to provide flexibility for integrated power and heat systems. Although not examined in this study, other sector coupling options exist including electric vehicles (EVs) and different power-to-X (P2X) conversion technologies, which couple the power sector with transport and industry sectors (see e.g. case studies of the Canary Islands [33], the Northern Europe [34] and Belgium [35]).

1.5. Contributions and paper structure

Many large scale power and energy system planning models still contain data in highly aggregated form (see e.g. a case study of U.S. [36] and the long-term planning model in a case study of Europe [37]), although there has also been focus in recent years to improve the accuracy of planning models [15]. The overall aim of this study is to analyse the impact of various temporal representations and operational details on generation expansion planning in energy systems, which are dominated by wind and solar energy, and to examine whether and how the impact varies depending on the system characteristics. The work involves a new time aggregation strategy, a new constraint to represent a combined reserve and rotational energy requirement, as well as a systematic evaluation of several investment planning model features and representations with a focus on the system specific nature of the impact of these decisions. The methodology and results provide important insights for modellers, who will increasingly need to incorporate higher levels of operational detail in planning models for future high VRE systems, while balancing with computational requirements.

The main contributions of this paper are the following:

- We compare the impacts of various temporal representations and operational details on investment planning in power and energy systems.
- We compare different methods for time series reduction and demonstrate the consequences of different ways to model storage state evolution. In addition to full year representation and representative week modelling with cyclic and continuous storage state assumptions, we propose a new aggregation strategy where a selected set of weeks is represented by a high resolution and the rest of the time horizon by a low resolution.
- We propose a new constraint to correctly represent the provision of very fast reserve products and rotational energy, important in future power systems with fewer online synchronous generators. Other operational details that are considered in this study are unit commitment decisions, FCR requirements and ramp limits with hourly and sub-hourly resolutions.
- We also examine the impact of modelling flexibility emerging from sector integration with different levels of detail, showing that appropriate modelling is crucial for analysing the value of flexibility provided by different technologies.
- In order to highlight the system-specific nature of the problem, we apply the methodology to two CO_2 price scenarios and to two test systems: a solar-dominated power system, and a wind-dominated power and district heat system.

The paper is organized as follows: Section 2 describes the applied modelling framework with mathematical formulations. Section 3 describes the test systems in the analysis as well as the temporal and operational detail cases. Section 4 presents the results, followed by a discussion in Section 5 and conclusion in Section 6.

2. Modelling framework

The case studies are carried out using the Backbone energy systems modelling tool [38] with unidirectionally soft-linked investment and operational models.

2.1. Approach

The optimization process selected for this study has two phases. First, the investment model is run in order to obtain optimal investment decisions, i.e., production (electricity and heat, in this study) and storage capacities. The capacities are fed into the operational model, which is then run in order to analyse the operational costs of the investment decisions. Fig. 1 depicts this process. The formulation of the investment model is varied in terms of the temporal representation and the operational details. By contrast, the formulation of the operational model stays the same, and only the capacity mix is altered according to the planning outcome of the investment model.

2.2. Model overview

The objective function (see Appendix A) minimizes all the eligible costs, including investment costs in the investment model and possible penalties for violating certain constraints. Compared to the model documentation [38], this study uses deterministic time series, and does not consider ramping costs, shutdown costs, or different start-up types (hot, warm, cold).

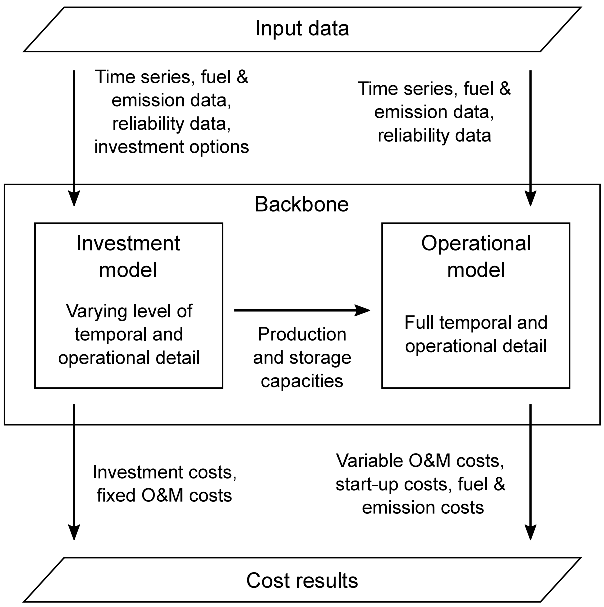

Fig. 1. The modelling approach consists of an investment model and an operational model, both implemented within the Backbone framework.

The model contains online variables that follow start-up and shutdown decisions, which are constrained, for example, by the minimum up and down times [38]. The efficiency representation that is used in this study is based on technology-clustered and continuously-relaxed online variables, which also enable a stylized representation of part-load efficiencies [38]. Relaxing all integer variables transforms the model into an LP model, which can be solved relatively easily. In this study, start-up and shutdown trajectories are disregarded. However, they become important especially with sub-hourly resolutions, and should be considered if very detailed results are required. In that case, the efficiency representation should also be more detailed, for example, using piecewise linear input–output curves without technology-based clustering and without relaxing the online variables.

Further detail on the formulation, such as the energy balance and ramping constraints, are given in [38]. In the following subsections, we describe further differences compared with our previous work [38].

2.3. Representing seasonal storage

In order to model seasonal storage, constraint (1) takes into account the weight of each sample, for example, if representing one year using 7 representative weeks.

$$\forall \{n, s', s\} \in NSS^{\text{bound}}, t = p_s^{\text{start}}, t' = p_{s'}^{\text{start}}, t'' = p_{s'}^{\text{end}} :$$

$$v_{n,t}^{\text{state}} = v_{n,t'}^{\text{state}} + p_{s'}^{\text{weight}} \left(v_{n,t''}^{\text{state}} - v_{n,t'}^{\text{state}} \right) \tag{1}$$

Constraint (1) is defined for each node n and sample pair $\{s', s\}$ that are joined in the three-dimensional set NSS^{bound}, so that the constraint holds for the starting time steps $t = p_s^{\text{start}}, t' = p_{s'}^{\text{start}}$ and ending time steps $t'' = p_{s'}^{\text{end}}$ of the samples. Parameters are denoted by p and variables by v. The $p_{s'}^{\text{weight}}$ parameter represents the weight of the sample. The variable $v_{n,t}^{\text{state}}$ is the node state (for example, hydro reservoir level).

2.4. Inertia requirement

The required amount of rotational energy in the system is based on the following general equation describing the RoCoF in the system (see e.g. [39]):

$$\frac{2H}{f_{\text{n}}} \frac{f_{\text{sys}}}{f_{\text{n}}} \frac{d f_{\text{sys}}}{dt} = \frac{\Delta P}{S_{\text{sys}}} \tag{2}$$

where H is the inertia constant, S_{sys} is the aggregated sum of apparent power, f_{n} is the nominal frequency, f_{sys} is the system frequency, $d f_{\text{sys}}/dt$ is the rate of change of the system frequency, and ΔP is the imbalance in the MW-power.

In the new version of Backbone, it is possible to let units contribute to the inertia requirement not only according to their rotational energy but also by very fast reserve provision, due to an increasing prevalence of fast frequency products [40]. In this study, we define two inertial reserve products $r \in R^{\text{inertia}}$, one ($p_{\omega,r}^{\text{reserve}} = 200$ MW) where both rotational energy of online machines and FFR from capable units can contribute, and another ($p_{\omega,r}^{\text{reserve}} = 50$ MW) where only rotational energy of online machines can contribute.

$$\forall \omega \in \Omega^{\text{inertiaReserve}}, r \in R^{\text{inertia}}, t \in T :$$

$$2 \times \underbrace{\Delta f_{\omega}}_{d f_{\text{sys}}/dt} \times \underbrace{\sum_{n \in N_{\omega}} \sum_{u \in U_n} p_{n,u}^{\text{inertia}} \times p_{n,u}^{\text{sizeMVA}} \times v_{u,t}^{\text{online}}}_{H \times S_{\text{sys}}}$$

$$\geq \underbrace{f_{\omega}^{0}}_{f_{\text{n}}} \times \left(\underbrace{p_{\omega,r}^{\text{reserve}}}_{\Delta P} - \sum_{n \in N_{\omega}} \sum_{u \in U_n} v_{r,n,u,t}^{\text{reserve}} \right) \tag{3}$$

Eq. (3) is a rewritten version of (2), with additional reserve provision that effectively decreases ΔP (see also [41]). In addition, we assume that $f_{\text{sys}} = f_{\text{n}}$. The constraint is defined separately for each group $\omega \in \Omega^{\text{inertiaReserve}}$ that joins nodes $n \in N_{\omega}$ and certain parameters, for each inertial reserve product $r \in R^{\text{inertia}}$ and time interval. In order to define an inertial reserve group, the user needs to define the default frequency (f_{ω}^{0}) in the associated nodes, the maximum RoCoF (Δf_{ω}), as well as the corresponding $p_{\omega,r}^{\text{reserve}}$ requirement — for example, the size of the largest unit in the system. Units connected to node n ($u \in U_n$) can contribute to the requirement according to their rotational energy or by providing the inertial reserve product in question. However, in the current setting, the same unit cannot contribute with both. Rotational energy is calculated based on the number of online sub-units ($v_{u,t}^{\text{online}}$), the MVA-capacity of a sub-unit ($p_{n,u}^{\text{sizeMVA}}$), and the inertia constant ($p_{n,u}^{\text{inertia}}$), given in seconds. The provision of the inertial reserve product is denoted by $v_{r,n,u,t}^{\text{reserve}}$, expressed in MW.

2.5. Modelling flexible CHP units

Flexibility in the output ratios of CHP technologies is modelled using the adaptable node-unit structure of the Backbone tool, see Fig. 2. The idea is similar to the one in [42] for representing a CHP plant using multiple conversion components in an energy systems model. Heat exchange losses in the district heat production are neglected but could be modelled by adding a node and a unit between the valve and the node representing the district heating load. The reactor and primary circuit of the nuclear-CHP are not modelled explicitly. Instead, they are included in the steam generator unit SG. Likewise, the gas turbine, heat recovery steam generator and high-pressure steam turbine of the NGCC-CHP are not modelled separately. Instead, they are all represented by the steam generator unit SG and turbine T1, which is followed by generator G1. A low-pressure steam turbine and its electricity production are represented by turbine-generator TG2.

In the Backbone framework, inputs and outputs of each conversion unit need to be calculated separately, and similarly, the balance at each node needs to be calculated separately. Below is a representation of the resulting functionalities for the nuclear-CHP technology using an artificial input and output variable v_i^{P}. The indices follow the same notation as in Fig. 2.

$$v_2^{\text{P}} = p_{\text{SG}}^{\text{eff}} v_1^{\text{P}} \tag{4}$$

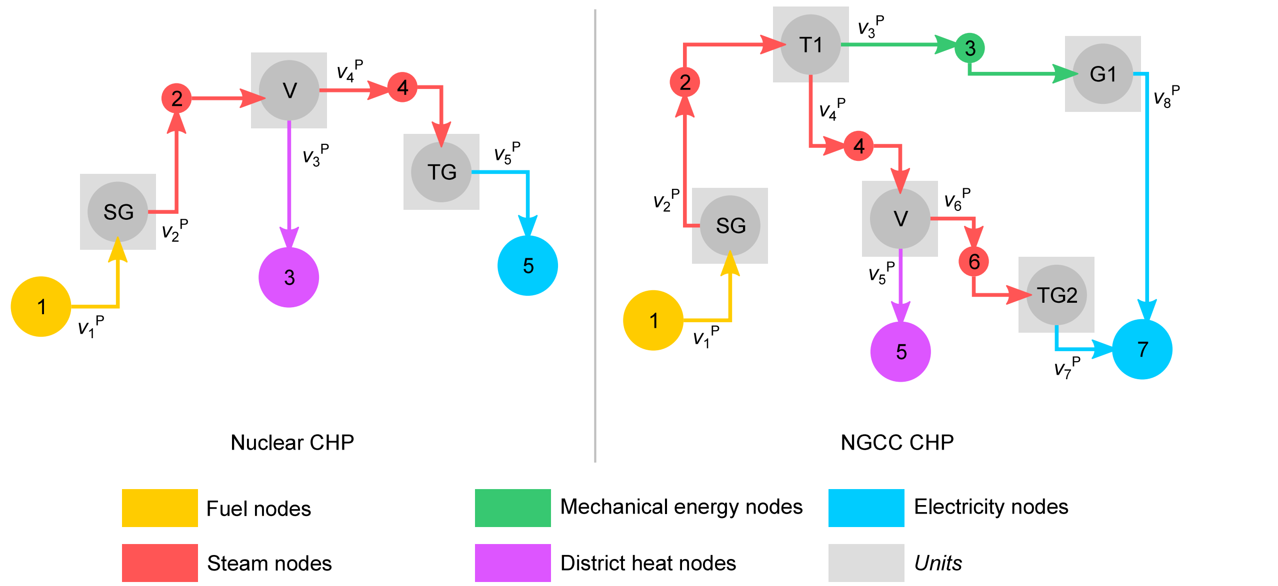

Fig. 2. Representation of the flexible CHP technologies using the node-unit structure of Backbone. CHP — combined heat and power, G — generator, NGCC — natural gas combined cycle, SG — steam generator, T — turbine, TG — turbine-generator, V — valve.

$$v_2^P = v_3^P + v_4^P \tag{5}$$

$$v_5^P = p_{TG}^{eff} v_4^P \tag{6}$$

$$p_V^{3,min} v_2^P \le v_3^P \le p_V^{3,max} v_2^P \tag{7}$$

$$p_{SG}^{min} v_{SG}^{online} \le v_2^P \le p_{SG}^{max} v_{SG}^{online} \tag{8}$$

$$p_{TG}^{min} v_{TG}^{online} \le v_5^P \le p_{TG}^{max} v_{TG}^{online} \tag{9}$$

where p_{SG}^{eff} and p_{TG}^{eff} represent the efficiency of steam generator SG and turbine-generator TG, respectively. The minimum and maximum operation levels of the those units are represented by parameters p_{SG}^{min}, p_{SG}^{max}, p_{TG}^{min}, and p_{TG}^{max}. Minimum and maximum operation levels are defined for turbine TG so that the unit would not provide unreasonable amounts of reserve. The $p_V^{3,max}$ parameter represents the maximum turbine bypass level (75% in this study), and $p_V^{3,min}$ is the minimum turbine bypass level (25% in this study).

A similar representation of the resulting functionalities is shown below for the NGCC-CHP technology. For the explanation of the indices, see Fig. 2.

$$v_2^P = p_{SG}^{eff} v_1^P \tag{10}$$

$$v_2^P = v_3^P + v_4^P \tag{11}$$

$$v_4^P = v_5^P + v_6^P \tag{12}$$

$$v_7^P = p_{TG2}^{eff} v_6^P \tag{13}$$

$$v_8^P = p_{G1}^{eff} v_3^P \tag{14}$$

$$v_3^P = p_{T1}^{fix} v_2^P \tag{15}$$

$$p_V^{5,min} v_4^P \le v_5^P \le p_V^{5,max} v_4^P \tag{16}$$

$$p_{SG}^{min} v_{SG}^{online} \le v_2^P \le p_{SG}^{max} v_{SG}^{online} \tag{17}$$

$$p_{G1}^{min} v_{G1}^{online} \le v_8^P \le p_{G1}^{max} v_{G1}^{online} \tag{18}$$

where p_{SG}^{eff}, p_{TG2}^{eff}, and p_{G1}^{eff} represent the efficiency of steam generator SG, turbine-generator TG2, and generator G1, respectively. The minimum and maximum operation levels of steam generator SG and generator G1 are represented by parameters p_{SG}^{min}, p_{SG}^{max}, p_{G1}^{min}, and p_{G1}^{max}. The p_{T1}^{fix} parameter stands for the mechanical efficiency of turbine T1 — a fixed proportion of thermal power input is converted to mechanical power output in turbine T1 and the rest is outputted as thermal power. The $p_V^{5,max}$ parameter represents the maximum steam extraction level after the high-pressure turbine (100% in this study), and $p_V^{5,min}$ is the minimum steam extraction level (0% in this study).

3. Case studies

The impact of operational details and temporal representations on generation expansion planning is analysed by applying investment and operational optimization to two test systems in a number of temporal and operational detail cases.

3.1. Test systems

Two greenfield test systems are used in this analysis: one based on the time series of the Reliability Test System Grid Modernization Lab Consortium (RTS-GMLC) [43] and another based on time series from Finland.

3.1.1. Time series

The test system based on the RTS-GMLC[4] contains one-year time series for correlated electric load, hydropower inflow, wind power capacity factor, photovoltaic (PV) capacity factor, and rooftop photovoltaic (RTPV) capacity factor. The resolution of the time series is 5 min.

The test system based on Finland contains one-year time series for correlated electric load, district heating load, hydropower inflow, wind power capacity factor, and PV capacity factor. The resolution of the time series is 1 h. The electric load profile is directly based on realized 2011 data,[5] while the profiles of the other time series categories were estimated based on 2011 weather data, technology assumptions, etc.

The analysis is based on deterministic modelling with perfect forecasts. In addition, we do not consider spatial detail, i.e., all time series categories are aggregated on a single node. Electric load is scaled linearly so that the peak is 10 GW, and district heating load and hydropower inflow are also scaled with the scale factor of electric load. Resulting average consumption levels and inflows as well as average capacity factors are shown in Table 1.

[4] https://github.com/GridMod/RTS-GMLC.

[5] https://www.fingrid.fi/en/electricity-market/electricity-market-information/load-and-generation/.

Table 1
Average capacity factor, inflow, and consumption data in the test systems.

System	Wind CF (%)	PV CF (%)	RTPV CF (%)	Hydro infl. (MW)	Elec. cons. (MW)	Heat cons. (MW)
RTS-GMLC (RTS)	31.1	26.1	20.1	583	5222	–
Finland (FIN)	34.8	8.9	–	270	6317	2314

Abbreviations: CF — capacity factor, PV — photovoltaic, RTPV — rooftop photovoltaic.

3.1.2. Technology, fuel and emission data

The analysis starts from a greenfield system without any initial production capacity. The investment model optimizes the power plant capacity investments from the set of candidate technologies, shown in Appendix B.

Two fuels are considered: natural gas and enriched uranium. The price of natural gas is assumed to be €36/MWh and the price of uranium is assumed to be €5/MWh. The CO_2 content of natural gas is 199.08 kg/MWh.

The CO_2 price varies between the scenarios from €0/tCO_2 to €100/tCO_2. The purpose is to create systems with different shares of low-carbon technologies and explore how the impact of the model configuration depends on the system. A similar effect could be achieved by varying the cost of low carbon technologies against the technologies utilizing natural gas, or by varying the natural gas price. The transport and storage cost for captured CO_2 is assumed to be €10/tCO_2.

3.1.3. Reliability

Reserve requirements and reserve provision are one of the operational details analysed in this study. We define three reserve categories:

- frequency containment reserve for normal operation (FCR-N), upward and downward: 3% of load + 5% of wind power generation + 5% of PV generation + 5% of RTPV generation
- frequency containment reserve for disturbances (FCR-D), upward: 200 MW
- fast frequency reserve (FFR), upward: 200 MW of which 50 MW has to come from the synchronous inertia of rotating machines in order to limit the RoCoF immediately after a large disturbance (assuming 50 Hz grid frequency and 0.5 Hz/s RoCoF)

For comparison, Barrows et al. [43] defined spinning reserve requirements as 3% of load. The selection of 200 MW for FCR-D and FFR is based on the assumed size of the largest possible unit in the system. However, it should be noted that these reserve requirements are examples and should not be interpreted as reserve levels that keep the test systems stable in all operational conditions. Actual reserve requirements in real systems should be determined based on thorough stability studies. The assumed reserve provision capabilities of the technologies are shown in Appendix B.

Furthermore, in the investment model, a capacity margin is defined for the electrical capacity for additional reliability reasons. It is assumed to be 10% of the peak load and it needs to be fulfilled for every time step in the model. Storage and VRE contribute to the capacity requirement according to their instantaneous production levels, and other technologies according to their installed electrical capacity. Heat pumps and electric boilers increase the electric load in the system and consequently also the capacity requirement according to their instantaneous consumption levels. Capacity margins and planning reserve margins are often used in investment models in order to ensure sufficient capacity. For example, Mai et al. [44] defined a planning reserve constraint that ensures that the total firm capacity must exceed the peak demand by 12.5%.

3.2. Cases

The case study configuration is based on unidirectionally soft-linked investment and operational models. First, the investment model is run in order to obtain optimal investments. Next, the operational model is run in order to analyse the operational feasibility and operational costs of the investment planning outcome.

For both test systems, we defined a number of cases with different temporal and operational detail in the investment model. The operational model always contained the full detail. Fig. 3 summarizes the set-up of the investment model in the different temporal and operational detail cases.

The features in the temporal representations of the investment model set-ups are further explained as follows.

- **full year**: Includes full one year time series at an hourly resolution and continuous modelling.
- **52wks**: Includes full year (less one day) time series at an hourly resolution, but instead of continuous modelling, the 52 weeks are modelled separately similar to representative weeks.
- **7wks**: Includes 7 weeks and 1–2 extreme days modelled at an hourly resolution. The number of extreme days depends on the presence of peak heat load (1 extreme day in the RTS-GMLC and 2 extreme days in the Finnish test system), and these days are selected using a two-stage approach similar to [6]. The total number of hourly time steps is 1200–1224. The weeks are treated as representative weeks, unless +aggr is mentioned in the set-up name. Representative weeks are selected instead of representative days in order to capture longer weather phenomena.
- **5wks**: Includes 5 weeks and 1–2 extreme days modelled at an hourly resolution. The extreme days are selected as described above. The weeks are treated as representative weeks, unless +aggr is mentioned in the set-up name.
- **/RD/**: The 5 or 7 weeks are selected from the full time series using regular decomposition [6].
- **/RS/**: The 5 or 7 weeks are selected from the full time series using random sampling [6].
- **+aggr**: Includes 5 or 7 selected weeks and 1–2 extreme days modelled at an hourly resolution. The rest of the year is modelled using aggregated 24-h time steps. The representation builds upon [9] but the selection of high-resolution and low-resolution time steps is directly based on the selection of representative weeks. The total number of time steps is 1193–1216 (5wks…+aggr), close to the number of time steps in the cases using 7 separately modelled representative weeks, or 1515–1538 (7wks…+aggr). Storage state evolves continuously.
- **unscaled**: The representative weeks are used as they appear in the one-year time series. Hence, the average capacity factor, inflow, and consumption data do not correspond exactly to the values in Table 1.
- **scaled**: The time series are linearly scaled so that the average capacity factor, inflow, and consumption data in the representative weeks correspond to the values in Table 1.
- **cyclic storage**: Storage state (hydropower reservoir and battery, as well as thermal storage in the Finnish test system) at the end of each sample (week or day) needs to be equal to the value at the beginning of the sample.

Temporal representation	Operational detail	Continuous full year using at least hourly resolution	Number of representative weeks	Number of high-resolution weeks (other weeks at daily resolution)	Scaled time series in repr. weeks (according to annual capacity factors)	Continuous (CO) or cyclic (CY) storage between repr. weeks	Repr. or high-resolution weeks selected using random sampling (RS) or regular decomposition (RD)	Highest resolution (1h, 15min, 5min)	Online variables	FCR requirement	FFR requirement	Ramp limits	Flexible output ratios of CHP units
unscaled, cyclic storage, 7wks/RD/	(no oper. details)	N	7	–	N	CY	RD	1h	N	N	N	N	N
unscaled, cyclic storage, 7wks/RS/	(no oper. details)	N	7	–	N	CY	RS	1h	N	N	N	N	N
scaled, cyclic storage, 7wks/RD/	(no oper. details)	N	7	–	Y	CY	RD	1h	N	N	N	N	N
scaled, cyclic storage, 7wks/RS/	(no oper. details)	N	7	–	Y	CY	RS	1h	N	N	N	N	N
	online							1h	Y	N	N	N	N
	online, FCR							1h	Y	Y	N	N	N
	online, FFR							1h	Y	N	Y	N	N
	online, FCR+FFR							1h	Y	Y	Y	N	N
	online, ramp limits							1h	Y	N	N	Y	N
	online, ramp limits, 15min							15min	Y	N	N	Y	N
	online, ramp limits, 5min							5min	Y	N	N	Y	N
	online, CHP flex							1h	Y	N	N	N	Y
scaled, continuous storage, 7wks/RS/	(no oper. details)	N	7	–	Y	CO	RS	1h	N	N	N	N	N
5wks/RS/+aggr	(no oper. details)	N	–	5	–	–	RS	1h	N	N	N	N	N
	online							1h	Y	N	N	N	N
	online, FCR							1h	Y	Y	N	N	N
	online, FFR							1h	Y	N	Y	N	N
	online, FCR+FFR							1h	Y	Y	Y	N	N
	online, ramp limits							1h	Y	N	N	Y	N
	online, ramp limits, 15min							15min	Y	N	N	Y	N
	online, ramp limits, 5min							5min	Y	N	N	Y	N
	online, CHP flex							1h	Y	N	N	N	Y
7wks/RS/+aggr	(no oper. details)	N	–	7	–	–	RS	1h	N	N	N	N	N
cyclic storage, 52wks	(no oper. details)	N	52	–	–	CY	–	1h	N	N	N	N	N
full year	(no oper. details)	Y	–	–	–	–	–	1h	N	N	N	N	N
	online							1h	Y	N	N	N	N
	online, FCR							1h	Y	Y	N	N	N
	online, FFR							1h	Y	N	Y	N	N
	online, FCR+FFR							1h	Y	Y	Y	N	N
	online, ramp limits							1h	Y	N	N	Y	N
	online, ramp limits, 15min							15min	Y	N	N	Y	N
	online, CHP flex							1h	Y	N	N	N	Y

Fig. 3. Set-up of the investment model in the temporal and operational detail cases. N — no; Y — yes.

- **continuous storage**: Storage state at the end of each sample needs to be equal to the value at the beginning of the next sample, taking into account the weighting of the representative weeks. Although the chronological order of the weeks in principle gets lost in the sampling, it is assumed that the representative weeks follow each other in the same order as they appear in the original time series.

The operational details that were considered in the investment model set-ups are explained as follows.

- **(no oper. details)**: Includes a simplified representation of the operational constraints in the investment model, where the following details are neglected: online variables, reserve requirements, ramp limits, sub-hourly timescales, and flexible CHP output ratios.
- **online**: Includes technology-clustered and continuously-relaxed online variables. Modelling also includes start-up and shutdown decision variables and costs, minimum up and down times, and a simple representation of part-load efficiencies.
- **FCR**: Includes FCR-N and FCR-D requirements.
- **FFR**: Includes synchronous inertia and FFR requirements.
- **ramp limits**: Includes ramp limits.
- **15min**: Includes a 15-min resolution for the periods which would otherwise be modelled at an hourly resolution (only RTS-GMLC).
- **5min**: Includes a 5-min resolution for the periods which would otherwise be modelled at an hourly resolution (only RTS-GMLC).
- **CHP flex**: Includes a possibility to vary CHP output ratios (only Finland).

The temporal and operational details were only varied in the investment model. In each temporal and operational detail case, the operational model uses a one-year rolling optimization with a one-year horizon, where the immediate time intervals have the highest resolution (5 min in the RTS-GMLC and 1 h in the Finnish test system) and the resolution gradually decreases towards the end of the horizon. The model rolls forward in 24-h steps. All the aforementioned operational details (online variables, reserve requirements, ramp limits, and flexible CHP output ratios) are considered in the operational model.

4. Results

This section provides the results of the case studies. As the focus of this paper is on the improvement of energy system models, the presented results are limited as follows. The cost impacts of the temporal and operational details are first analysed separately, and then, the analysis is further justified by exploring the planning outcomes. The computation times of the investment models are also compared.

4.1. Cost impacts of temporal representations

As expected, including full year time series in the investment model, either using 52 separate weeks or full continuous time series, resulted in the lowest costs. The other temporal representations have different advantages and disadvantages depending on the test system, as shown in Fig. 4. Based on a literature review [15], there is no standard approach to manage temporal detail in large scale power and energy system planning models. Thus, all cases in Fig. 4 are compared to the 'full year' case, which has the highest level of detail. The RTS-GMLC cases with representative weeks selected by the regular decomposition method show remarkably high costs compared to the corresponding cases with weeks selected by the random sampling method. By contrast, in the Finnish cases, the regular decomposition selection proved to perform slightly better than random sampling selection. This highlights that the performance of different representative period selection methods varies depending on the system. Changing the cyclic storage level constraints to seasonal ones did not have noticeable effect on costs in either test system, which was rather surprising given the strong seasonality in the Finnish data. It may be that the pre-defined hydro reservoirs, the batteries and the thermal storage technology were not optimal for such long-term storage that the continuous storage level modelling would have had large impacts. Furthermore, the modelling accuracy would have benefitted from storage level checks at regular intervals [11].

Representing 5 or 7 selected weeks using an hourly resolution and the rest of the year using a daily resolution proved to be a relatively reliable time series reduction method for the wind-dominated Finnish test system with high seasonal variation in electricity and heat consumption. Furthermore, the CO_2 price had no noticeable impact on its suitability. The benefit of this representation is that the behaviour of medium- and long-term storage can be better captured, while the flexibility needs caused by high-resolution variations are visible in the 5 or 7 selected weeks. However, in the solar-dominated RTS-GMLC test system, the same aggregation method increased the costs outstandingly by roughly 30%–50% compared to the full year case. This highlights the natural conclusion that especially in a solar-dominated system, aggregating a large part of the time series to 24-h time steps significantly underestimates the short-term flexibility needs of the system. The short-term flexibility needs are also underestimated in a wind-dominated system, but not to the same extent.

Rather consistently, the cost impacts were larger in the cases where the CO_2 price was set at a higher level. At higher CO_2 prices and increasing levels of variable renewable energy, the need to consider more operational situations in the investment planning model becomes higher, and thus a larger part of the full time series should be included.

4.2. Cost impacts of operational details

Fig. 5 shows the results when operational details were added on top of the following three cases: 'scaled, cyclic storage, 7wks/RS/', '5wks/RS/+aggr', and 'full year'. All operational detail cases are compared to the corresponding '(no oper. details)' case, which can be considered a standard approach for large scale energy system planning models [15]. In the case of the RTS-GMLC system, the impact of operational details was not significant, and most of that impact resulted from simply including online variables and the corresponding start-up and shutdown decisions and costs. There were relatively large differences in the operational detail cases based on '5wks/RS/+aggr', but the results are not reliable as the temporal representation itself was unsuitable for the system.

In the Finnish cases, the highest benefits were achieved in the cases that considered online variables together with flexible output ratios of CHP units. The benefits varied in the range of 0.3%–1.4%, depending on the CO_2 price. Modelling the interactions of different energy sectors and the true flexibility of sector coupling technologies plays a more critical role when the share of VRE is high. Including the FCR and FFR requirements in the investment model also showed clear benefits especially in the '5wks/RS/+aggr' case. Interestingly, including online variables in the investment model slightly increased the costs of the Finnish test system in the 'scaled, cyclic storage, 7wks/RS/' case. In order to avoid start-up costs, the model with online variables may invest more in units with low start-up costs but potentially high fixed or variable costs instead of units with high start-up costs. However, if the selected weeks in the investment planning model contain a high variation compared to the full time series, hence overestimating the level of plant cycling required, the investments into the units with low start-up costs may prove to be oversized and costly in the operational phase. The random sampling method for selecting representative periods in this study did not consider variability.

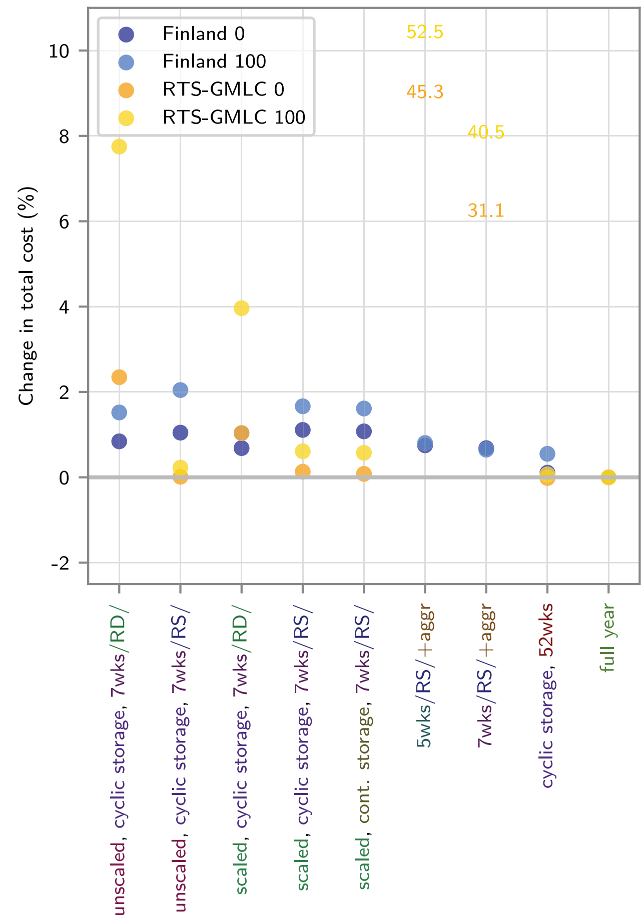

Fig. 4. Impact of temporal representations on annual system costs. All cases are compared to the 'full year' case. CO_2 price €0 per tonne or €100 per tonne.

4.3. Capacity results

Reasons for the cost differences can be seen in the capacity results in Figs. 6–7. In the RTS-GMLC cases, the generation portfolios are largely the same within the CO_2 price scenarios, except for the cases based on the '5wks/RS/+aggr' and '7wks/RS/+aggr' representation. Those cases resulted in significantly lower battery and wind power capacities as well as higher OCGT and PV capacities compared to the other cases. The investment planning model assumed that it would need to use the OCGTs mainly during the 5 or 7 weeks that were modelled with a high resolution, whereas PV capacity would be able to handle the consumption during the rest of the year mainly alone. The cases based on regular decomposition selections also had less battery capacity and less PV capacity compared to the other cases. It is important that variations and correlations of the time series are correctly captured. Using a 15-min or 5-min resolution in the investment model did not have a considerable impact on the planning outcome, as the hourly model already resulted in a significant amount of flexible battery capacity. The impact could be very different when using an inflexible existing system as a starting point, instead of the greenfield approach.

In the Finnish cases, there is also more variation in the capacity results between the different operational detail cases. For example, considering the flexible output ratios of CHP plants in the investment planning model resulted in more NGCC-CHP plants, whereas the capacity of NGCC and gas boilers decreased. In the high CO_2 price scenario, the model started to invest in nuclear-CHP plants, while omitting investments in heat pumps. Nuclear-CHP plants and heat pumps (as well as nuclear heat plants) are competing technologies as they both

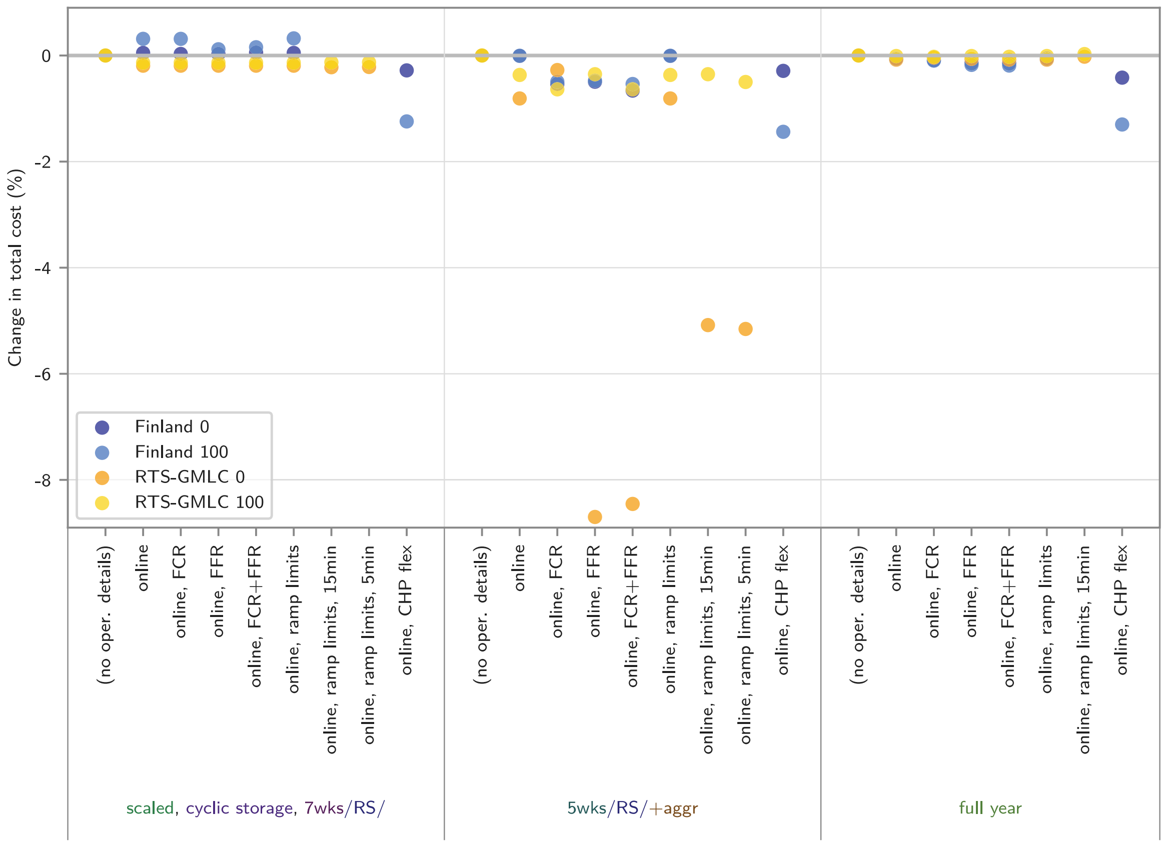

Fig. 5. Impact of operational details on annual system costs. All cases are compared to the corresponding '(no oper. details)' case. CO_2 price €0 per tonne or €100 per tonne.

require a relatively large number of full load hours to be cost-effective. At the same time, electric boiler capacity, thermal storage capacity, and wind power capacity also decreased. As was noticed in the RTS-GMLC cases, battery capacity also decreased when using the '5wks/RS/+aggr' and '7wks/RS/+aggr' representation in the Finnish test system. The benefits of short-term storage are underestimated when representing a large part of the time series using a very coarse resolution. However, compared to the separately modelled representative weeks, the capacity of thermal storage increased when using the partly aggregated, continuous temporal representations in the high CO_2 price scenario, becoming close to the full year results. Thus, the benefits of relatively long-term storage are better captured when considering continuous time series, even if a large part of the time series is modelled at a very coarse resolution.

4.4. Computation time

Fig. 8 shows how the computation time increases when including more operational details and more time steps in the investment model. The magnitude of the impact of additional details on the computation time is often different in the Finnish system and the RTS-GMLC. This result also highlights that the sensitivity of the model to the different configurations partly depends on the system.

In general, adding more time steps, either by moving to sub-hourly resolutions or by including full hourly time series instead of selected days or weeks, quickly slowed down the solution process. Adding relaxed online variables had a clear impact on the solution time, especially in the Finnish system, whereas the different reserve categories often played a smaller role on the speed of the solution process. The detailed modelling of CHP flexibility did not impact the computation time much, partly because the CHP units were modelled using the rather complicated network structure in all cases (see Fig. 2). In the flexible CHP cases, the valve units were just modelled using inequality constraints instead of equality constraints. In the slowest cases, the model features increased the solution time over 400 times (Finland) or over 600 times (RTS-GMLC) compared to the fastest solution, which was 'unscaled, cyclic storage, 7wks/RD/'.

5. Discussion

Investment planning models and other energy system tools are frequently used by academia and industry to inform policy makers, energy utilities, transmission system operators, investors and manufactures about how climate targets can be reached and what particular technologies will be the most valuable in a particular system or region. Improved models will give more accurate results and higher quality information to support decision making.

The results demonstrate that the best method for sampling representative periods can change between systems. Similarly, the level of operational detail that should be included at the planning stage depends on the system. This indicates that it can be worthwhile to test multiple methods and parametrizations before settling on one of them for a particular use case. In the authors' opinion, a modelling framework could benefit from a testing machinery that can be applied whenever a model is being applied for a particular purpose.

The results indicate that a more detailed representation of energy sector coupling can significantly impact the planning outcomes. In our example, giving the CHP units more control over heat and power outputs resulted in considerably cheaper total system costs. While this is only one example, the interactions between the energy sectors can often have complex constraints and their impact for the planning stage needs to be understood better, in order not to over- or underestimate their ability to help the system in various operational challenges.

Start-up and shutdown trajectories of power plants were not considered. This could have had an impact especially in the RTS-GMLC system, which had a 5-min resolution in the operational stage. On the

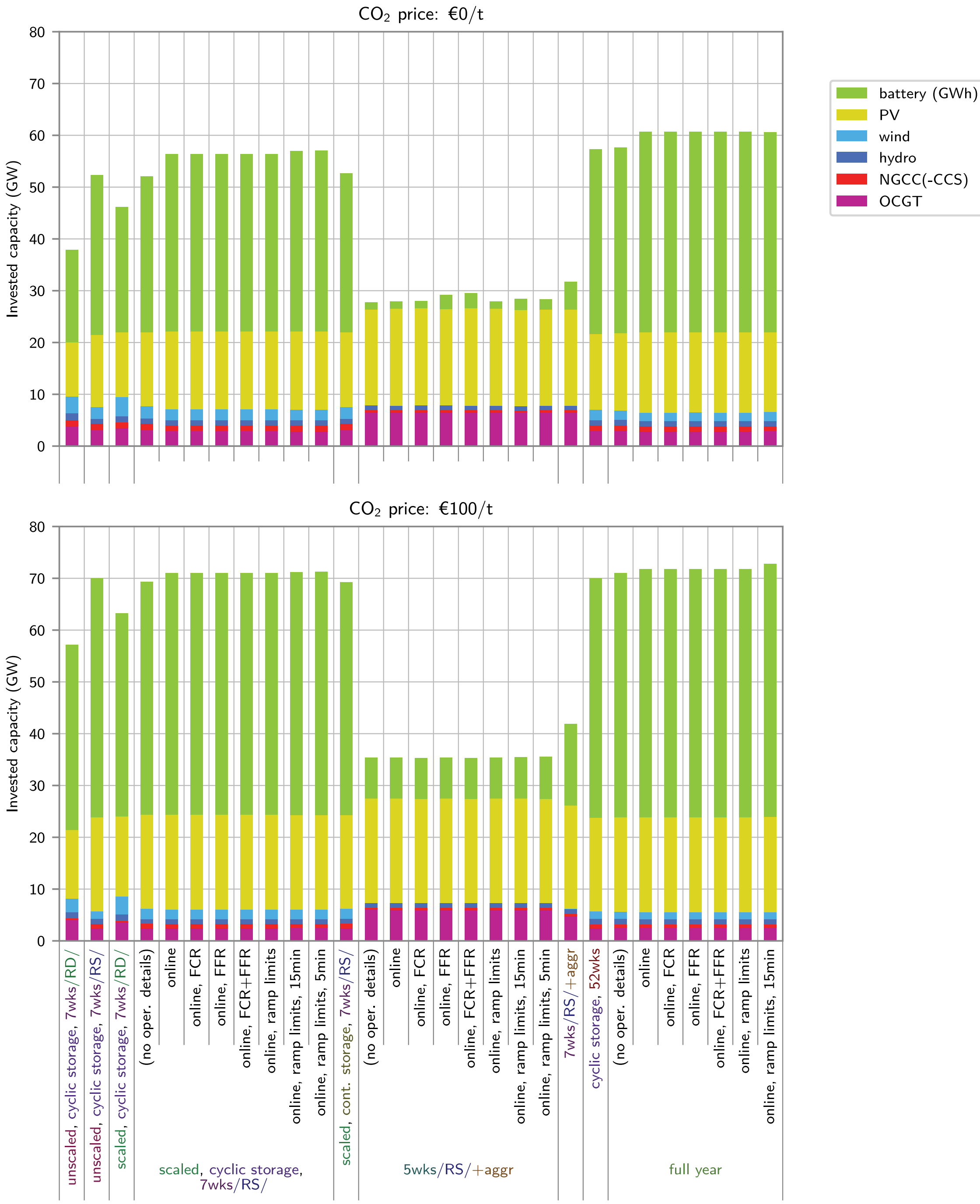

Fig. 6. Invested capacity in the RTS-GMLC cases with different temporal representations and operational details.

other hand, almost all of the RTS-GMLC cases had a significant amount of flexible battery capacity in the results which may have been able to compensate for the slower start-up and shutdown times of some other units. The only cases that did not have a significant amount of battery capacity were the ones that represented a large portion of the year using 24-h time steps, which was not a suitable temporal representation for a solar-dominated power system. The representation could be improved by increasing the granularity of the low-resolution periods, but this would increase the total number of time steps unless the number of days modelled at high resolution were simultaneously reduced.

The cost assumptions likely have a significant impact on the planning outcomes. As the study did not include sensitivity analysis on the cost assumptions, the reader should be careful when making far-reaching interpretations of the relative importance of the technologies. Moreover, the test systems consisted of a single node and reserve sizing was not verified through detailed technical simulations. While consideration of these aspects would be of importance in actual power and energy system planning, more comprehensive modelling was not undertaken as part of this study, allowing for detailed analysis of the impacts of temporal representations and operational details.

When applying the improvements in models depicting real power and energy systems, data availability can become an issue. In addition, real systems are often linked to neighbouring systems, and appropriate modelling of these links and systems complicates both data management and model calculation. Some regions and sectors may need to be modelled using lower detail in order to overcome these complications.

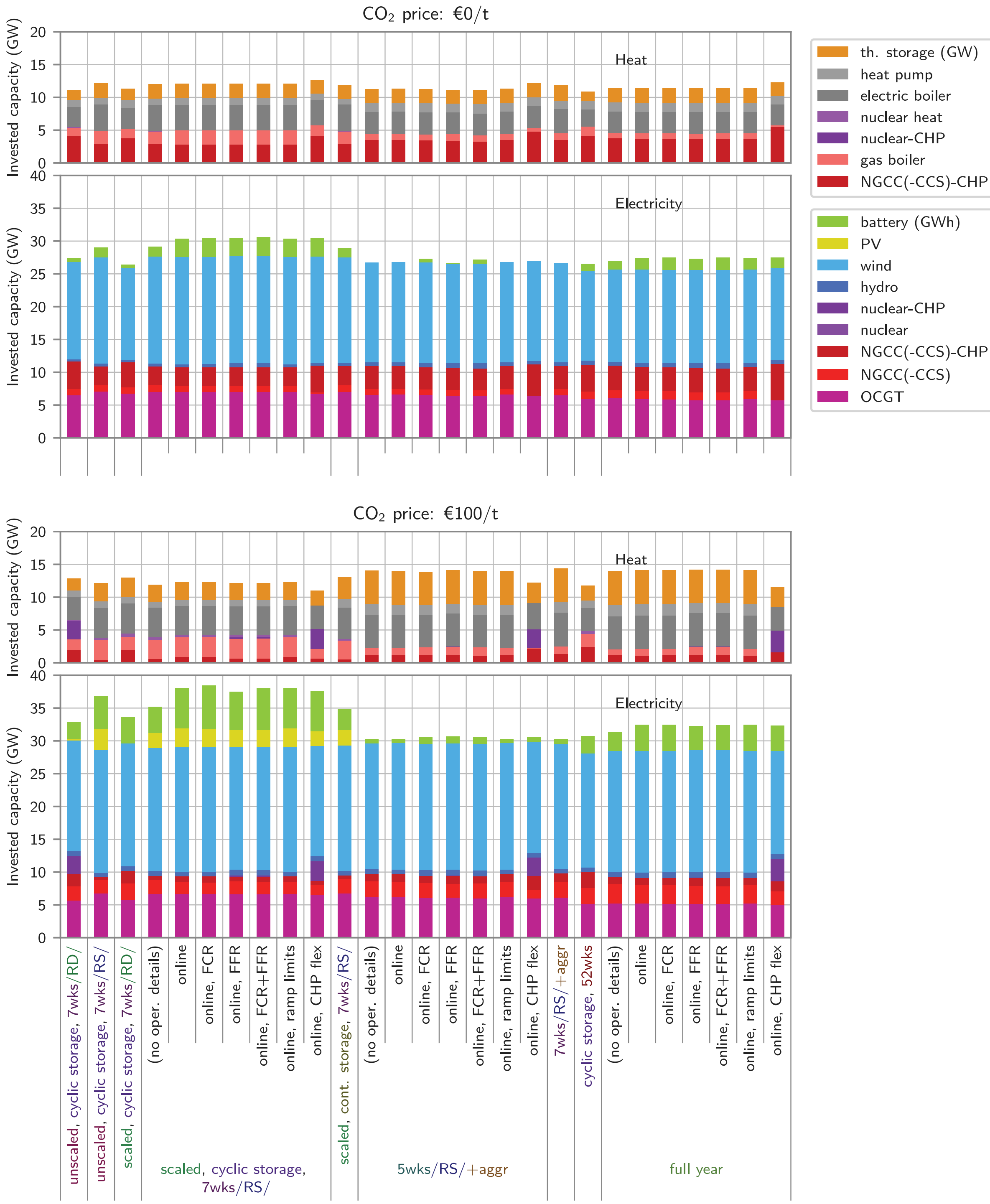

Fig. 7. Invested capacity in the Finnish cases with different temporal representations and operational details.

6. Conclusion

This study showed how temporal representations and operational details in the investment planning stage affect the total costs and planning outcomes of energy systems dominated by wind and solar energy. While some methods better capture the needs and behaviour of long-term storage, they may at the same time underestimate the need for short-term storage, and vice versa. These findings provide information about the advantages and disadvantages of different model configurations as well as foundations for forming an initial selection of configurations for different systems. However, based on the results, the use of testing machinery is recommended in order to find the most suitable configuration whenever the system under study changes significantly or the purpose of the study changes. The links to different energy sectors are important to capture, and the coupling technologies should be properly modelled already in the investment planning stage — that is, their flexibility should not be over- or underestimated. When reaching towards 100% renewable power and energy systems, there may be enough inherent variability in the variable renewable energy time series to encourage flexibility investments, and some operational

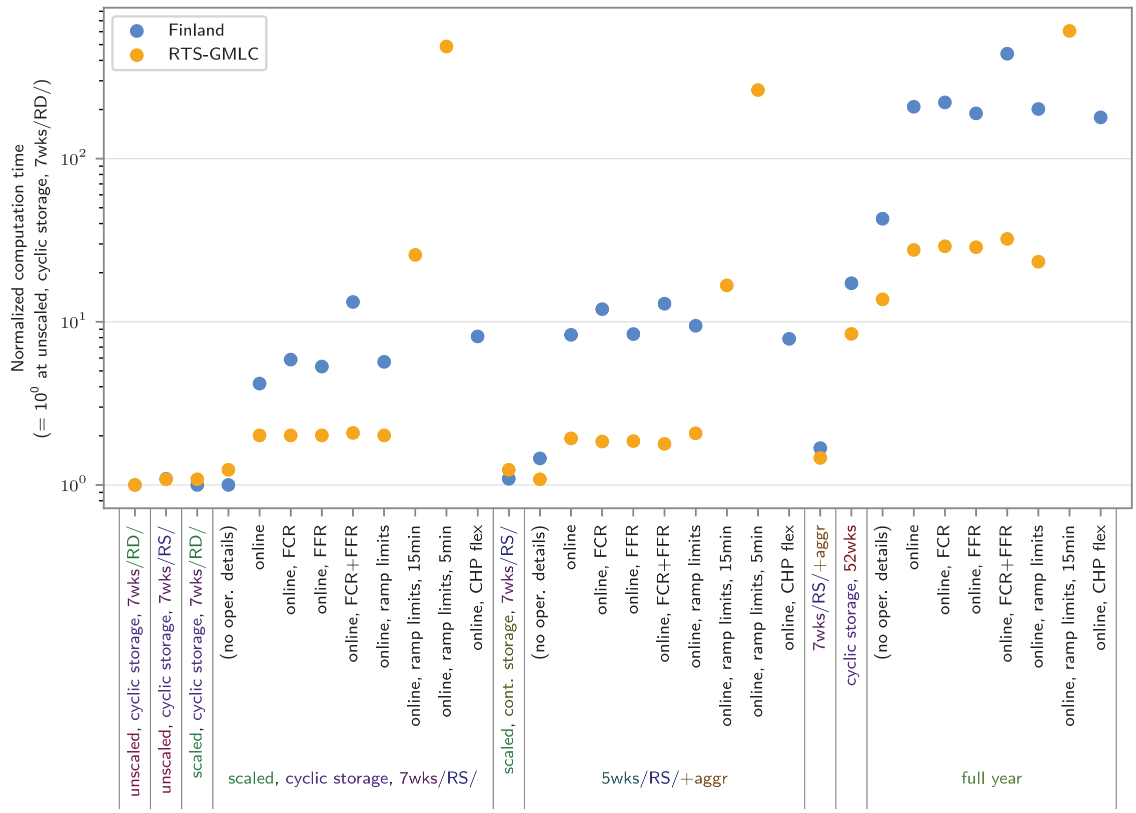

Fig. 8. Impact of temporal representations and operational details on the average duration of the investment model runs. Note the logarithmic scale.

details that have been important at medium variable renewable energy shares, such as start-up and shutdown characteristics, may start to lose their significance in the investment planning stage. In contrast, at increasing levels of variable renewable energy, the need to consider more operational situations (e.g., different weather conditions) and challenges in the planning stage becomes higher, and thus the models need to include more time steps.

CRediT authorship contribution statement

Niina Helistö: Conceptualization, Methodology, Software, Validation, Formal analysis, Investigation, Data curation, Writing - original draft, Writing - review & editing, Visualization, Funding acquisition. **Juha Kiviluoma:** Conceptualization, Methodology, Software, Writing - review & editing, Supervision, Project administration, Funding acquisition. **Germán Morales-España:** Writing - review & editing. **Ciara O'Dwyer:** Methodology, Software, Writing - review & editing.

Acknowledgements

N.H. has received funding from the Jenny and Antti Wihuri Foundation. This work has been supported by the Strategic Research Council at the Academy of Finland, project "Transition to a Resource Efficient and Climate Neutral Electricity System (EL-TRAN)" (grant number 314319). This project has received funding from the European Union's Horizon 2020 research and innovation programme under grant agreement No 864276. Ciara O'Dwyer has received funding from the European Union Horizon 2020 research and innovation programme under grant agreement No 774629.

Appendix A. Objective function

The objective function (A.1) is a simplified version of the one presented in [38].

$$\min\left(\sum_{t\in T} p_t^{\text{probability}} \times \left(v_t^{\text{vomCost}} + v_t^{\text{fuelCost}} + v_t^{\text{startupCost}} + v_t^{\text{penalties}}\right) + v^{\text{stateValueDecrease}} + v^{\text{fomCost}} + v^{\text{unitInvestCost}}\right) \tag{A.1}$$

where $t \in T$ includes the time intervals in the model, and $p_t^{\text{probability}}$ is the total probability and weight of the time interval, taking into account the weight of the samples (e.g., representative days and weeks). Parameters are denoted by p and variables by v.

The variable operational and maintenance (O&M) costs v_t^{vomCost} and fuel and emissions costs v_t^{fuelCost} are defined as

$$v_t^{\text{vomCost}} = \Delta_t \times \sum_{n\in N}\sum_{u\in U_n} p_{n,u}^{\text{vomCost}} \times v_{n,u,t}^{\text{gen}} \tag{A.2}$$

$$v_t^{\text{fuelCost}} = \Delta_t \times \sum_{u\in U}\sum_{h\in H_u^{\text{main}}} \left(p_h^{\text{fuelPrice}} + \sum_{e\in E_h} p_{h,e}^{\text{fuelEmission}} \times \frac{\sum_{n\in N} p_{e,n}^{\text{emissionTax}} \times p_{n,u}^{\text{size}}}{\sum_{n\in N} p_{n,u}^{\text{size}}}\right) \times v_{h,u,t}^{\text{fuelUse}} \tag{A.3}$$

The duration of the time interval is represented with Δ_t, set $n \in N$ includes all the nodes in the model, $u \in U$ includes all the energy conversion units in the model, and $u \in U_n$ includes all the units that have output or input capacity at node n. Fuels used by unit u are included in $h \in H_u^{\text{main}}$ and emissions caused by fuel h are in $e \in E_h$. Parameters $p_{n,u}^{\text{vomCost}}$ and $p_{n,u}^{\text{size}}$ represent the variable O&M costs in €/MWh and the MW-capacity of the unit, respectively. If the unit consists of several identical sub-units, $p_{n,u}^{\text{size}}$ denotes the MW-capacity of

Table B.1
Technical parameters for electricity-only technologies.
Source: Adapted from [21,45–52].

Type (fuel)	Unit size elec. (MW_e)	Unit size apparent (MVA)	Efficiency (min.) (%)	Efficiency (max.) (%)	Min. load (%)	Ramp up/ down limit (%/min)	Inertia constant (s)	Min. up/ down time (h)
Wind	1	–	100	100	0	–	–	–
PV	1	–	100	100	0	–	–	–
RTPV	1	–	100	100	0	–	–	–
Hydro	100	111	100	100	0	–	2.4	–
OCGT (NG)	50	56	40	45	20	40	5.29	1
NGCC (NG)	200	222	58	63	40	5	4.97	1
NGCC-CCS (NG)	181	222	51	56	40	5	4.97	1
Nuclear (U)	57	63	28.5	28.5	40	0.67	4.07	24
Battery	160[a]	–	92	92	0	–	–	–
Synchronous condenser	−3[b]	100	100	100	100	–	2	–

Abbreviations: PV — photovoltaic, RTPV — rooftop photovoltaic, OCGT — open cycle natural gas turbine, NGCC — natural gas combined cycle, CCS — carbon capture and storage, NG — natural gas, U — uranium.
Hydropower storage capacity is fixed to 24 GWh in the test systems.
CCS technology is assumed to have a CO_2 capture rate of 90%.
[a]For battery technology, the unit of measurement for unit size is MWh. A battery with a capacity of 160 MWh is assumed to have a 80-MW charging capability and a 480-MW discharging capability.
[b]Negative values denote that the technology consumes electricity.

a sub-unit. Parameters $p_h^{\text{fuelPrice}}$, $p_{h,e}^{\text{fuelEmission}}$, and $p_{e,n}^{\text{emissionTax}}$ represent the fuel price (€/MWh), emission content of the fuel (kg/MWh), and the price of the emission (€/kg), respectively. Variables $v_{n,u,t}^{\text{gen}}$ and $v_{h,u,t}^{\text{fuelUse}}$ represent the output of the unit (or input if < 0) and the fuel use, respectively, both in MW.

Start-up costs $v_t^{\text{startupCost}}$ are:

$$v_t^{\text{startupCost}} = \sum_{u \in U^{\text{online}}} p_u^{\text{startupCost}} \times v_{u,t}^{\text{startup}} \tag{A.4}$$

where $u \in U^{\text{online}}$ includes all the units with online variables, $p_u^{\text{startupCost}}$ represents start-up costs in €/sub-unit, and $v_{u,t}^{\text{startup}}$ is the start-up decision variable, expressed in the number of sub-units.

Penalties $v_t^{\text{penalties}}$ result from the slack variables which allow violations on the energy balance, reserve requirement, and capacity margin constraints:

$$\begin{aligned} v_t^{\text{penalties}} = \Delta_t \times \sum_{n \in N} \Bigg(& p_n^{\text{balanceSlackPenalty}} \times \left(v_{n,t}^{\text{slackUp}} + v_{n,t}^{\text{slackDown}} \right) \\ & + \sum_{r \in R} \left(p_r^{\text{reserveSlackPenalty}} \times v_{r,n,t}^{\text{reserveSlack}} \right) \\ & + p_n^{\text{capacitySlackPenalty}} \times v_{n,t}^{\text{capacitySlack}} \Bigg) \end{aligned} \tag{A.5}$$

The energy balance equality has slack variables applied to both directions ($v_{n,t}^{\text{slackUp}}$ and $v_{n,t}^{\text{slackDown}}$), while the reserve requirement and capacity margin inequalities only need slack variables in one direction ($v_{r,n,t}^{\text{reserveSlack}}$ and $v_{n,t}^{\text{capacitySlack}}$, respectively). The set $r \in R$ represents different reserve categories. The penalties are set to the following values:

- $p_n^{\text{balanceSlackPenalty}}$ =€20 000/MWh
- $p_r^{\text{reserveSlackPenalty}}$ =€40 000/MWh
- $p_n^{\text{capacitySlackPenalty}}$ =€10 000/MWh

Changes in the economic value of the node states (storage) $v^{\text{stateValueDecrease}}$ are calculated as follows:

$$v^{\text{stateValueDecrease}} = \sum_{n \in N} \left(p_{n,t^{\text{start}}}^{\text{stateValue}} \times v_{n,t^{\text{start}}}^{\text{state}} - p_{n,t^{\text{end}}}^{\text{stateValue}} \times v_{n,t^{\text{end}}}^{\text{state}} \right) \tag{A.6}$$

At the beginning of the model horizon, the state (for example, hydro reservoir level) is $v_{n,t^{\text{start}}}^{\text{state}}$, and at the end $v_{n,t^{\text{end}}}^{\text{state}}$. The state can have a different economic value at the beginning ($p_{n,t^{\text{start}}}^{\text{stateValue}}$) and at the end of the horizon ($p_{n,t^{\text{end}}}^{\text{stateValue}}$). The unit of measurement of the states can be selected freely. Assuming it MWh, the unit of its economic value would be €/MWh.

Table B.2
Economic parameters for electricity-only technologies.
Source: Adapted from [45–47,52–56].

Type	CAPEX (€/kW_e)	FOM (€/kW_e/a)	VOM (€/MWh_e)	Start cost (€/MW_e)
Wind	960	11.34	1.22	0
PV	560	7.40	0	0
RTPV	490	7.81	0	0
Hydro	1264	11.34	1.22	0
OCGT	412	7.423	4.50	43
NGCC	800	26.00	4.00	64.5
NGCC-CCS	1784	45.50	7.00	64.5
Nuclear	4000	100.00	4	64.5
Battery	135[a]	1.62[a]	1.60[a]	0
Synchronous condenser	2825	16.96	0	1290

Abbreviations: CAPEX — capital expenditure, FOM — fixed operational and maintenance costs, VOM — variable operational and maintenance costs, PV — photovoltaic, RTPV — rooftop photovoltaic, OCGT — open cycle natural gas turbine, NGCC — natural gas combined cycle, CCS — carbon capture and storage.
The same annuity factor 0.0944 is used for all units, calculated as $\frac{r}{1-(1+r)^{-n}}$, where $r = 7\%$ and $n = 20$.
[a]For battery technology, the units of measurement for investment costs and fixed O&M costs are €/kWh and €/kWh/a, respectively. Variable O&M costs are calculated from the discharged energy.

Fixed O&M costs v^{fomCost} and unit investment costs $v^{\text{unitInvestCost}}$ are calculated as follows:

$$v^{\text{fomCost}} = \sum_{n \in N} \sum_{u \in U_n} p_{n,u}^{\text{fomCost}} \times p_{n,u}^{\text{size}} \times v_u^{\text{invest}} \tag{A.7}$$

$$v^{\text{unitInvestCost}} = \sum_{n \in N} \sum_{u \in U_n} p_{n,u}^{\text{investCost}} \times p_{n,u}^{\text{annuity}} \times p_{n,u}^{\text{size}} \times v_u^{\text{invest}} \tag{A.8}$$

Parameters $p_{n,u}^{\text{fomCost}}$, $p_{n,u}^{\text{investCost}}$, and $p_{n,u}^{\text{annuity}}$ represent the fixed O&M costs, investment costs, and the annuity factor of the energy conversion unit, given in €/MW/a, €/MW, and 1/a, respectively. Parameter $p_{n,u}^{\text{size}}$ denotes the MW-capacity of a sub-unit. Variable v_u^{invest} represents the investment decision, expressed in the number of invested sub-units. Here, we relax this variable in order to avoid forcing the solution into the stepwise capacity increments based on the pre-defined sub-unit sizes.

Table B.3
Technical parameters for electricity and heat technologies.
Source: Adapted from [45–49,51,52].

Type (fuel)	Unit size elec. (MW_e)	Unit size heat (MW_{dh})	Unit size apparent (MVA)	Efficiency (min.) (%)	Efficiency (max.) (%)	Min. load (%)	Ramp up/ down limit (%/min)	Inertia constant (s)	Min. up/ down time (h)
NGCC-CHP (NG)	100	72.1	111	89.5	94.5	40	5	4.97	1
NGCC-CCS-CHP (NG)	89	72.1	111	83.8	88.5	40	5	4.97	1
Gas boiler (NG)	–	10	–	104	106	15	–	–	–
Nuclear-CHP (U)	45	50	50	47.5	47.5	40	0.67	4.07	24
Nuclear heat (U)	–	200	–	100	100	40	0.67	–	24
Electric boiler	−10[b]	10	–	100	100	5	–	–	–
Heat pump	−0.98[b]	4	–	410	410	10	–	–	–
Thermal storage[a]	–	4500[a]	–	100	100	0	–	–	–

Abbreviations: NGCC — natural gas combined cycle, CCS — carbon capture and storage, CHP — combined heat and power, NG — natural gas, U — uranium.
CCS technology is assumed to have a CO_2 capture rate of 90%.
[a]For thermal storage technology, the unit of measurement for unit size is MWh. A thermal storage facility with a capacity of 4500 MWh is assumed to have a 30-MW charging capability and a 30-MW discharging capability. The self-discharge rate of thermal storage is assumed to be 0.01 $MWh/d/MWh_{state}$, i.e. without any charging and discharging the storage state will decrease to half of its original value in 69 days.
[b]Negative values denote that the technology consumes electricity.

Table B.4
Technical parameters for CHP technologies in an alternative production mode.

Type	Unit size elec. (MW_e)	Unit size heat (MW_{dh})	Efficiency (min.) (%)	Efficiency (max.) (%)
NGCC-CHP[a]	110.8	0	57.6	60.8
NGCC-CCS-CHP[a]	99.8	0	51.3	54.8
nuclear-CHP[b]	15	150	82.5	82.5

Abbreviations: NGCC — natural gas combined cycle, CCS — carbon capture and storage, CHP — combined heat and power.
[a]In the alternative mode of NGCC-CHP and NGCC-CCS-CHP, steam from high-pressure turbine is directed to low-pressure turbine in order to replace district heat production with more electricity generation.
[b]In the alternative mode of nuclear-CHP, the steam turbine is bypassed more in order to replace electricity generation with more district heat production.

Appendix B. Technology data

The characteristics of the candidate technologies are shown in Tables B.1, B.2, B.3, B.4, and B.5. The cost and other parameters are not trying to represent actual values accurately — rather, the studied technologies and their parameter values serve to demonstrate the value of operational detail in investment planning. Likewise, the uncertainty of cost and other technology parameters was not considered in this study, allowing for detailed analysis of the impacts of temporal representations and operational details. The technologies in Tables B.3, B.4, and B.5 are only available in the Finnish test system that contains district heating consumption. The CHP technologies are assumed to have a flexible ratio between heat and power production. The ratio in one extreme is presented in Table B.3, and in another extreme in Table B.4. The technologies can also produce heat and power in a ratio between the presented extremes.

Table B.6
Reserve provision capabilities as percentage of the available capacity.

Type	FCR-N (%)	FCR-D (%)	FFR (%)
Wind[a]	20	20	20
PV[a]	20	20	20
Hydro	100	100	0
OCGT	20	20	0
NGCC	15	0	0
NGCC-CCS	15	0	0
Nuclear	2	0	0
Battery	100	100	100
NGCC-CHP	15	0	0
NGCC-CCS-CHP	15	0	0
Nuclear-CHP	2	0	0
Electric boiler	100	100	100
Heat pump	20	10	0

Abbreviations: FCR-N — frequency containment reserve for normal operation, FCR-D — frequency containment reserve for disturbances, FFR — fast frequency reserve, PV — photovoltaic, RTPV — rooftop photovoltaic, OCGT — open cycle natural gas turbine, NGCC — natural gas combined cycle, CCS — carbon capture and storage, CHP — combined heat and power.
The values are own estimates, partly based on [45] and the ramp limits in Tables B.1 and B.3.
[a]Reserve provision capability is calculated from the available capacity, i.e. it depends on the capacity factor time series. The relatively low value of 20% is selected for the wind and PV units in order to reflect the assumption that not all units will be participating in reserve provision.

Table B.5
Economic parameters for electricity and heat technologies.
Source: Adapted from [45–47,52,54].

Type	CAPEX		FOM		VOM		Start cost	
	(€/∗)	∗	(€/∗/a)	∗	(€/∗)	∗	(€/∗)	∗
NGCC-CHP	1100	kW_e	26.00	kW_e	4.00	MWh_e	37.5	MW_{th}
NGCC-CCS-CHP	1925	kW_e	45.50	kW_e	7.00	MWh_e	37.5	MW_{th}
Gas boiler	50	kW_{dh}	1.70	kW_{dh}	1.00	MWh_{dh}	0	
Nuclear-CHP	5067	kW_e	126.70	kW_e	1.20	MWh_{th}	14.5	MW_{th}
Nuclear heat	1000	kW_{dh}	28.50	kW_{dh}	1.20	MWh_{th}	7.25	MW_{th}
Electric boiler	60	kW_{dh}	0.92	kW_{dh}	1.00	MWh_{dh}	0	
Heat pump	530	kW_{dh}	2.00	kW_{dh}	3.90	MWh_{dh}	0	
Thermal storage	0.47	kWh_{th}	0.003	kWh_{th}	0		0	

Abbreviations: CAPEX — capital expenditure, FOM — fixed operational and maintenance costs, VOM — variable operational and maintenance costs, NGCC — natural gas combined cycle, CCS — carbon capture and storage, CHP — combined heat and power.
Subscripts: dh — district heat output, e — electricity output, th — thermal capacity of the whole unit.
The same annuity factor 0.0944 is used for all units, calculated as $\frac{r}{1-(1+r)^{-n}}$, where $r = 7\%$ and $n = 20$.

Table B.6 shows the reserve provision capabilities of the technologies. Technologies that are not in Table B.6 cannot provide any reserve but may be able to provide synchronous inertia according to their inertia constant and apparent power (see Tables B.1 and B.3).

References

[1] Scott IJ, Carvalho PM, Botterud A, Silva CA. Clustering representative days for power systems generation expansion planning: Capturing the effects of variable renewables and energy storage. Appl Energy 2019;253:113603. http://dx.doi.org/10.1016/j.apenergy.2019.113603.

[2] Poncelet K, Höschle H, Delarue E, Virag A, D'haeseleer W. Selecting representative days for capturing the implications of integrating intermittent renewables in generation expansion planning problems. IEEE Trans Power Syst 2017;32(3):1936–48. http://dx.doi.org/10.1109/TPWRS.2016.2596803.

[3] Palmintier B, Bugbee B, Gotseff P. Representative day selection using statistical bootstrapping for accelerating annual distribution simulations. In: 2017 IEEE power and energy society innovative smart grid technologies conference, ISGT 2017. Washington, DC, USA; 2017, p. 1–5, http://dx.doi.org/10.1109/ISGT.2017.8086066.

[4] Pfenninger S. Dealing with multiple decades of hourly wind and PV time series in energy models: A comparison of methods to reduce time resolution and the planning implications of inter-annual variability. Appl Energy 2017;197:1–13. http://dx.doi.org/10.1016/j.apenergy.2017.03.051.

[5] de Sisternes FJ, Webster MD. Optimal selection of sample weeks for approximating the net load in generation planning problems. ESD working paper series ESD-WP-2013-03, Massachusetts Institute of Technology Engineering Systems Division; 2013.

[6] Helistö N, Kiviluoma J, Reittu H. Selection of representative slices for generation expansion planning using regular decomposition. Energy 2020;211:118585. http://dx.doi.org/10.1016/j.energy.2020.118585.

[7] Hilbers AP, Brayshaw DJ, Gandy A. Importance subsampling: improving power system planning under climate-based uncertainty. Appl Energy 2019;251:113114. http://dx.doi.org/10.1016/j.apenergy.2019.04.110.

[8] Yeganefar A, Amin-Naseri MR, Sheikh-El-Eslami MK. Improvement of representative days selection in power system planning by incorporating the extreme days of the net load to take account of the variability and intermittency of renewable resources. Appl Energy 2020;272:115224. http://dx.doi.org/10.1016/j.apenergy.2020.115224.

[9] Pineda S, Morales JM. Chronological time-period clustering for optimal capacity expansion planning with storage. IEEE Trans Power Syst 2018;33(6):7162–70. http://dx.doi.org/10.1109/TPWRS.2018.2842093.

[10] Wogrin S, Tejada-Arango DA, Pineda S, Morales JM. What time-period aggregation method works best for power system operation models with renewables and storage?. In: 2019 international conference on smart energy systems and technologies (SEST). Porto, Portugal: IEEE; 2019, p. 1–6. http://dx.doi.org/10.1109/SEST.2019.8849027.

[11] Tejada-Arango DA, Domeshek M, Wogrin S, Centeno E. Enhanced representative days and system states modeling for energy storage investment analysis. IEEE Trans Power Syst 2018;33(6):6534–44. http://dx.doi.org/10.1109/TPWRS.2018.2819578.

[12] Kotzur L, Markewitz P, Robinius M, Stolten D. Time series aggregation for energy system design: Modeling seasonal storage. Appl Energy 2018;213:123–35. http://dx.doi.org/10.1016/j.apenergy.2018.01.023.

[13] Morales-España G, Tejada-Arango DA. Modeling the hidden flexibility of clustered unit commitment. IEEE Trans Power Syst 2019;34(4):3294–6. http://dx.doi.org/10.1109/TPWRS.2019.2908051.

[14] Gaur AS, Das P, Jain A, Bhakar R, Mathur J. Long-term energy system planning considering short-term operational constraints. Energy Strategy Rev 2019;26:100383. http://dx.doi.org/10.1016/j.esr.2019.100383.

[15] Helistö N, Kiviluoma J, Holttinen H, Lara JD, Hodge B-M. Including operational aspects in the planning of power systems with large amounts of variable generation: a review of modeling approaches. WIREs Energy Environ 2019;1–34. http://dx.doi.org/10.1002/wene.341.

[16] Poncelet K, Delarue E, D'haeseleer W. Unit commitment constraints in long-term planning models: Relevance, pitfalls and the role of assumptions on flexibility. Appl Energy 2020;258:113843. http://dx.doi.org/10.1016/j.apenergy.2019.113843.

[17] Commission Regulation (EU) 2017/1485 of 2 August 2017 establishing a guideline on electricity transmission system operation (Text with EEA relevance.). 2017, URL: http://data.europa.eu/eli/reg/2017/1485/oj.

[18] Nycander E, Söder L, Olauson J, Eriksson R. Curtailment analysis for the Nordic power system considering transmission capacity, inertia limits and generation flexibility. Renew Energy 2020;152:942–60. http://dx.doi.org/10.1016/j.renene.2020.01.059.

[19] Matevosyan J, Badrzadeh B, Prevost T, Quitmann E, Ramasubramanian D, Urdal H, et al. Grid-forming inverters: Are they the key for high renewable penetration?. IEEE Power Energy Mag 2019;17(6):89–98. http://dx.doi.org/10.1109/MPE.2019.2933072.

[20] Wogrin S, Tejada-Arango D, Delikaraoglou S, Botterud A. Assessing the impact of inertia and reactive power constraints in generation expansion planning. Appl Energy 2020;280:115925. http://dx.doi.org/10.1016/j.apenergy.2020.115925.

[21] Nguyen HT, Yang G, Nielsen AH, Jensen PH. Combination of synchronous condenser and synthetic inertia for frequency stability enhancement in low-inertia systems. IEEE Trans Sustain Energy 2019;10(3):997–1005. http://dx.doi.org/10.1109/TSTE.2018.2856938.

[22] Thakurta PG, Flynn D. Network studies for a 100% converter-based power system. J Eng 2019;2019(18):5250–4. http://dx.doi.org/10.1049/joe.2018.9253.

[23] Morales-España G, Lorca Á, de Weerdt MM. Robust unit commitment with dispatchable wind power. Electr Power Syst Res 2018;155:58–66. http://dx.doi.org/10.1016/j.epsr.2017.10.002.

[24] Hodge B-MS, Jain H, Brancucci C, Seo G-S, Korpås M, Kiviluoma J, et al. Addressing technical challenges in 100% variable inverter-based renewable energy power systems. WIREs Energy Environ 2020;9(5):e376. http://dx.doi.org/10.1002/wene.376.

[25] O'Dwyer C, Flynn D. Using energy storage to manage high net load variability at sub-hourly time-scales. IEEE Trans Power Syst 2015;30(4):2139–48. http://dx.doi.org/10.1109/TPWRS.2014.2356232.

[26] Palmintier B. Flexibility in generation planning: Identifying key operating constraints. In: 2014 power systems computation conference. 2014, p. 1–7. http://dx.doi.org/10.1109/PSCC.2014.7038323.

[27] Schwele A, Kazempour J, Pinson P. Do unit commitment constraints affect generation expansion planning? A scalable stochastic model. Energy Syst 2020;11(2):247–82. http://dx.doi.org/10.1007/s12667-018-00321-z.

[28] Priesmann J, Nolting L, Praktiknjo A. Are complex energy system models more accurate? An intra-model comparison of power system optimization models. Appl Energy 2019;255:113783. http://dx.doi.org/10.1016/j.apenergy.2019.113783.

[29] IRENA. Global renewables outlook: Energy transformation 2050. Technical report, Abu Dhabi, United Arab Emirates: International Renewable Energy Agency (IRENA); 2020, URL: www.irena.org/publications.

[30] Levihn F. CHP and heat pumps to balance renewable power production: Lessons from the district heating network in Stockholm. Energy 2017;137:670–8. http://dx.doi.org/10.1016/j.energy.2017.01.118.

[31] Guelpa E, Verda V. Thermal energy storage in district heating and cooling systems: A review. Appl Energy 2019;252:113474. http://dx.doi.org/10.1016/j.apenergy.2019.113474.

[32] Bach B, Werling J, Ommen T, Münster M, Morales JM, Elmegaard B. Integration of large-scale heat pumps in the district heating systems of Greater Copenhagen. Energy 2016;107:321–34. http://dx.doi.org/10.1016/j.energy.2016.04.029.

[33] Gils HC, Simon S. Carbon neutral archipelago – 100% renewable energy supply for the Canary Islands. Appl Energy 2017;188:342–55. http://dx.doi.org/10.1016/j.apenergy.2016.12.023.

[34] Ikäheimo J, Kiviluoma J, Weiss R, Holttinen H. Power-to-ammonia in future North European 100 % renewable power and heat system. Int J Hydrogen Energy 2018;43(36):17295–308. http://dx.doi.org/10.1016/j.ijhydene.2018.06.121.

[35] Berger M, Radu D, Fonteneau R, Deschuyteneer T, Detienne G, Ernst D. The role of power-to-gas and carbon capture technologies in cross-sector decarbonisation strategies. Electr Power Syst Res 2020;180:106039. http://dx.doi.org/10.1016/j.epsr.2019.106039.

[36] Jayadev G, Leibowicz BD, Kutanoglu E. U.S. electricity infrastructure of the future: Generation and transmission pathways through 2050. Appl Energy 2020;260:114267. http://dx.doi.org/10.1016/j.apenergy.2019.114267.

[37] Pavičević M, Mangipinto A, Nijs W, Lombardi F, Kavvadias K, Jiménez Navarro JP, et al. The potential of sector coupling in future European energy systems: Soft linking between the Dispa-SET and JRC-EU-TIMES models. Appl Energy 2020;267:115100. http://dx.doi.org/10.1016/j.apenergy.2020.115100.

[38] Helistö N, Kiviluoma J, Ikäheimo J, Rasku T, Rinne E, O'Dwyer C, et al. Backbone—an adaptable energy systems modelling framework. Energies 2019;12(17):3388. http://dx.doi.org/10.3390/en12173388.

[39] Hartmann B, Vokony I, Táczi I. Effects of decreasing synchronous inertia on power system dynamics—Overview of recent experiences and marketisation of services. Int Trans Electr Energy Syst 2019;29(12):e12128. http://dx.doi.org/10.1002/2050-7038.12128.

[40] Eriksson R, Modig N, Elkington K. Synthetic inertia versus fast frequency response: A definition. IET Renew Power Gener 2018;12(5):507–14. http://dx.doi.org/10.1049/iet-rpg.2017.0370.

[41] Badesa L, Teng F, Strbac G. Simultaneous scheduling of multiple frequency services in stochastic unit commitment. IEEE Trans Power Syst 2019;34(5):3858–68. http://dx.doi.org/10.1109/TPWRS.2019.2905037.

[42] Lindroos TJ, Rydén M, Langørgen Ø, Pursiheimo E, Pikkarainen T. Robust decision making analysis of BECCS (bio-CLC) in a district heating and cooling grid. Sustain Energy Technol Assess 2019;34:157–72. http://dx.doi.org/10.1016/j.seta.2019.05.005.

[43] Barrows C, Bloom A, Ehlen A, Ikäheimo J, Jorgenson J, Krishnamurthy D, et al. The IEEE reliability test system: A proposed 2019 update. IEEE Trans Power Syst 2020;35(1):119–27. http://dx.doi.org/10.1109/TPWRS.2019.2925557.

[44] Mai T, Drury E, Eurek K, Bodington N, Lopez A, Perry A. Resource planning model: An integrated resource planning and dispatch tool for regional electric systems. Technical report, Golden, CO, USA: National Renewable Energy Laboratory (NREL); 2013, URL: https://www.nrel.gov/docs/fy13osti/56723.pdf.

[45] Danish Energy Agency and Energinet. Technology data for energy plants for electricity and district heating generation. Technical report, Copenhagen, Denmark: Danish Energy Agency and Energinet; 2019, URL: https://ens.dk/en/our-services/projections-and-models/technology-data/technology-data-generation-electricity-and.

[46] Danish Energy Agency and Energinet. Technology data for energy storage. Technical report, Copenhagen, Denmark: Danish Energy Agency and Energinet; 2019, URL: https://ens.dk/en/our-services/projections-and-models/technology-data/technology-data-energy-storage.

[47] Irlam L. Global costs of carbon capture and storage: 2017 update. Technical report, Global CCS Institute; 2017.

[48] EPRI. Advanced nuclear technology: advanced light water reactor utility requirements document, revision 13. Technical report, Electric Power Research Institute (EPRI); 2014, URL: https://www.epri.com/{#}/pages/product/3002003129/.

[49] Sahlberg V. Pienreaktorit kaukolämmön tuotannossa. 2019, Presentation at "Kaukolämpöpäivät", 29/08/2019.

[50] Nambiar M, Konstantinovic Z. Impact of using synchronous condensers for power system stability and improvement of short-circuit power in mining projects. Min Eng 2015;67(1):38–44.

[51] Johnson SC, Papageorgiou DJ, Mallapragada DS, Deetjen TA, Rhodes JD, Webber ME. Evaluating rotational inertia as a component of grid reliability with high penetrations of variable renewable energy. Energy 2019;180:258–71. http://dx.doi.org/10.1016/j.energy.2019.04.216.

[52] Schröder A, Friedrich K, Meiss J, Mendelevitch R, von Hirschhausen C. Data documentation 68: Current and prospective costs of electricity generation until 2050. Technical report, Berlin, Germany: DIW Berlin; 2013, p. 1–94, URL: https://www.diw.de/documents/publikationen/73/diw{_}01.c.424566.de/diw{_}datadoc{_}2013-068.pdf.

[53] IRENA. Renewable power generation costs in 2018. Technical report, Abu Dhabi, United Arab Emirates: International Renewable Energy Agency (IRENA); 2019, URL: www.irena.org/publications.

[54] Zero Emissions Platform. The costs of CO2 capture, transport and storage: Post-demonstration CCS in the EU. Technical report, European Technology Platform for Zero Emission Fossil Fuel Power Plants; 2011, URL: www.zeroemissionsplatform.eu.

[55] Igbinovia FO, Fandi G, Müller Z, Švec J, Tlusty J. Cost implication and reactive power generating potential of the synchronous condenser. In: 2016 2nd international conference on intelligent green building and smart grid (IGBSG). Prague, Czech Republic; 2016, p. 1–6. http://dx.doi.org/10.1109/IGBSG.2016.7539450.

[56] GDH. AEMO costs and technical parameter review: Report Final Rev 4. Technical report, Australian Energy Market Operator (AEMO); 2018.